Scholars Journal of Engineering and Technology
OPEN ACCESS
Abbreviated Key Title: Sch J Eng Tech
ISSN 2347-9523 (Print) | ISSN 2321-435X (Online)
Journal homepage: https://saspublishers.com

A Density Functional Theory Investigation of the Fragmentation Mechanism of Deprotonated Serine

Quan Sun[1*], Hongjie Qu[1], Qiang Li[1], Dongxue Ding[1], Lili Cao[1], Jingyu Pang[1], Siyu Xia[1]

[1]College of Science, Heilongjiang Bayi Agricultural University, Daqing, 163319, Heilongjiang Province, P. R. China

DOI: 10.36347/sjet.2022.v10i07.008 | **Received:** 11.06.2022 | **Accepted:** 25.07.2022 | **Published:** 27.07.2022

***Corresponding author:** Quan Sun
College of Science, Heilongjiang Bayi Agricultural University, Daqing, 163319, Heilongjiang Province, P. R. China

Abstract **Original Research Article**

In this paper, density functional theory (DFT) was applied to study the dissociation process of NH_3- and H_2O-loss reaction of the deprotonate serine ([Ser–H]$^-$) at BH*and*HLYP/6-31G level. The geometric structure of the isomers, transition states and dissociation products of [Ser–H]$^-$ was optimized. The related energy of the material was obtained by frequency calculation, and the potential energy profile of NH_3- and H_2O-loss reaction was constructed. The possibility and direction of the reaction along different paths were discussed. It is indicated that the stable structure of [Ser–H]$^-$ is **1d**. In the NH_3-loss reaction path, the optimal structure of proton serine isomer is **2j**, and the dominant channel is **Path 6**. The Gibbs energy of the corresponding ration-determined step is 61.88 kcal·mol^{-1}. The optimal structure of [Ser–H]$^-$ isomer in H_2O-loss reaction is **1i**, and its dominant channel is **Path 7**. The Gibbs activation energy of the corresponding ration-determining step is 74.15 kcal·mol^{-1}. It can be seen that NH_3-loss reaction is easier than H_2O-loss reaction under this reaction condition.

Keywords: Deprotonate serine, reaction mechanism, H_2O-loss reaction, NH_3-loss reaction.

1. INTRODUCTION

Serine is a non-charged and non-essential ketogenic amino acid in 20 common amino acids of protein, which can be used as a modification group of protein [1]. The discovery of serine dates back to 1865, when Cramer hydrolyzed the sericin component of silk protein with sulfuric acid, then hydrolyzed it and discovered that sweet crystals could be extracted. In 1880, Erlenmeyer proposed the crystal structure of the sweet taste, suggesting that the structure of the compound was α-amino-β hydroxypropionic acid [2]. Serine can be broken down into glycine and one carbon unit. In living organisms, one carbon unit is necessary for the synthesis of nucleotides and methylation [3], which occurs through the production of methionine, which is the main source of carbon units in cancer cells [4]. From this point of view, serine is metabolically necessary and plays an important role in some cellular processes. Therefore, regulation of serine metabolism in mammalian tissues is crucial for the control of methyl transfer.

Bowie [5] investigated the cleavage of deprotonated amino acids and peptides using fast atomic bombardment (FAB) tandem mass spectrometry. Piraud [6] observed deamination of [Ser−H]$^-$ in mass spectrometry to form molecular ion fragment [Ser−H−NH_3]$^-$. Eckersley [7] found that [Ser−H]$^-$ could not only remove ammonia molecules to form molecular fragment [Ser−H−NH_3]$^-$, but also remove water molecules to form molecular fragment [Ser−H−H_2O]$^-$ by tandem mass spectrometry using FAB.

In this paper, the mechanism of NH_3- and H_2O-loss reaction of [Ser−H]$^-$ was investigated at BH*and*HLYP/6-31G level. The geometry of all [Ser−H]$^-$ isomers, transition states, cleavage product molecules and ions are optimized. By calculating the frequency, the total electron energy, enthalpy and Gibbs free energy of each structure and the relative total electron energy, enthalpy change and Gibbs free energy of each reaction path are obtained, and the potential energy profile constituted by the reaction is constructed accurately [8-10]. Based on the above data, the spontaneous direction and difficulty degree of the reaction process were discussed from the perspective of chemical thermodynamics and kinetics respectively, and the optimal path of [Ser−H]$^-$ cleavage could be found. The results can provide some model support for the cleavage mechanism of other deprotonated amino acid ions.

2. COMPUTATIONAL DETAILS

The geometric configurations of all reactants, intermediates, transition states, products and dissociated neutral molecules were obtained by using BH*and*HLYP method [11-19] combined with 6-31G base set [20-22] in corporated in the Gaussian09 program system [23]. After geometric optimization, frequency vibration calculation is carried out to determine the geometrical position is the minimum value (no virtual frequency) or transition state (only one virtual frequency). In addition, we also calculate the thermal correction of the key stability points at the same level in geometric optimization, and obtain their relative enthalpy of reaction and Gibbs free energy of relative reaction.

3. RESULT AND DISCUSSION

3.1 Isomerization of [Ser−H]$^-$

There is a chiral carbon atom based on [Ser−H]$^-$, and all models are left-handed deprotic serine. The geometric structures of 46 isomers were optimized and searched in this paper. According to the different positions of negative charge, they can be divided into four types. The corresponding structures are shown in Figure 1, and the related energies are listed in Table 1.

Table 1: Enthalpy (H, *a.u.*), Gibbs free energy (G, *a.u.*) and Relative Gibbs free energy (ΔG, in kcal·mol^{-1}) of each stagnation point obtained of the isomerization process of [Ser−H]$^-$

Names	H	G	ΔG	Names	H	G	ΔG
1a	-397.920672	-397.959842	2.62	**3c**	-397.820358	-397.859463	65.61
1b	-397.917183	-397.956633	4.63	**3d**	-397.807776	-397.847617	70.36
1c	-397.905303	-397.945586	8.88	**3e**	-397.794440	-397.835648	80.55
1d	-397.925391	-397.964014	0.00	**3f**	-397.794209	-397.835153	80.86
1e	-397.920573	-397.959745	2.68	**3g**	-397.787847	-397.845907	74.11
1f	-397.907253	-397.947402	10.42	**3h**	-397.793531	-397.834267	81.42
1g	-397.915184	-397.958632	3.38	**3i**	-397.788912	-397.839678	78.02
1h	-397.915299	-397.954491	5.98	**3j**	-397.792504	-397.833448	81.93
1i	-397.907251	-397.947402	7.75	**3k**	-397.809188	-397.849362	71.95
2a	-397.856082	-397.907091	35.72	**3l**	-397.794734	-397.849757	71.70
2b	-397.859802	-397.899535	40.46	**3m**	-397.793504	-397.834450	81.30
2c	-397.856824	-397.897695	41.62	**3n**	-397.825392	-397.854013	69.03
2d	-397.862990	-397.904019	37.65	**4a**	-397.879075	-397.897516	41.73
2e	-397.865845	-397.906784	35.91	**4b**	-397.850036	-397.890352	46.22
2f	-397.873230	-397.913568	31.66	**4c**	-397.858873	-397.898565	41.07
2g	-397.872052	-397.913237	31.86	**4d**	-397.859146	-397.898328	41.22
2h	-397.865143	-397.905233	36.89	**4e**	-397.858059	-397.897707	41.61
2i	-397.873232	-397.906572	36.05	**4f**	-397.862207	-397.901779	39.05
2j	-397.874382	-397.908275	34.98	**4g**	-397.847305	-397.908116	35.08
2k	-397.864148	-397.906228	36.26	**4h**	-397.848930	-397.910062	33.86
2l	-397.866084	-397.905236	36.88	**4i**	-397.853634	-397.893217	41.75
3a	-397.792171	-397.833146	82.12	**4j**	-397.860966	-397.900471	39.87
3b	-397.798124	-397.838743	78.61	**4k**	-397.879071	-397.907417	35.52

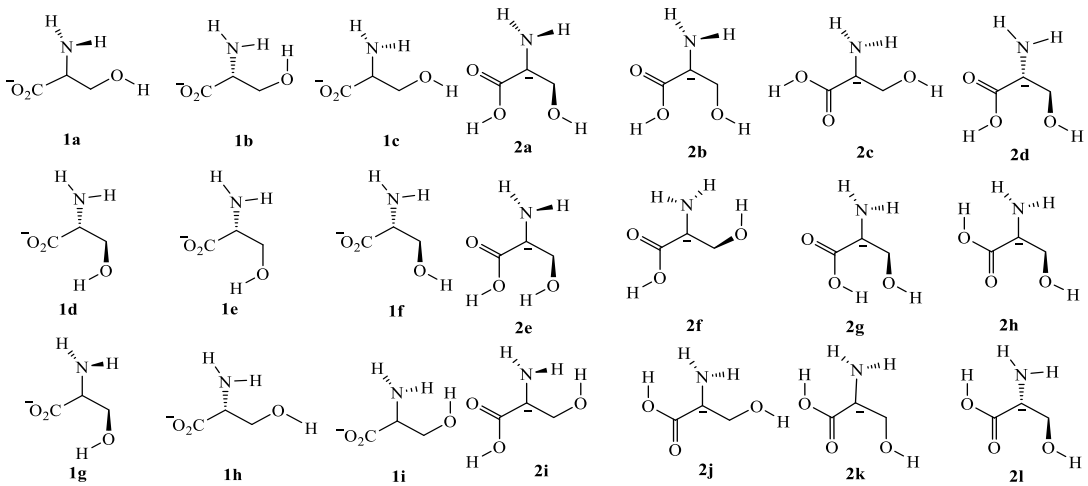

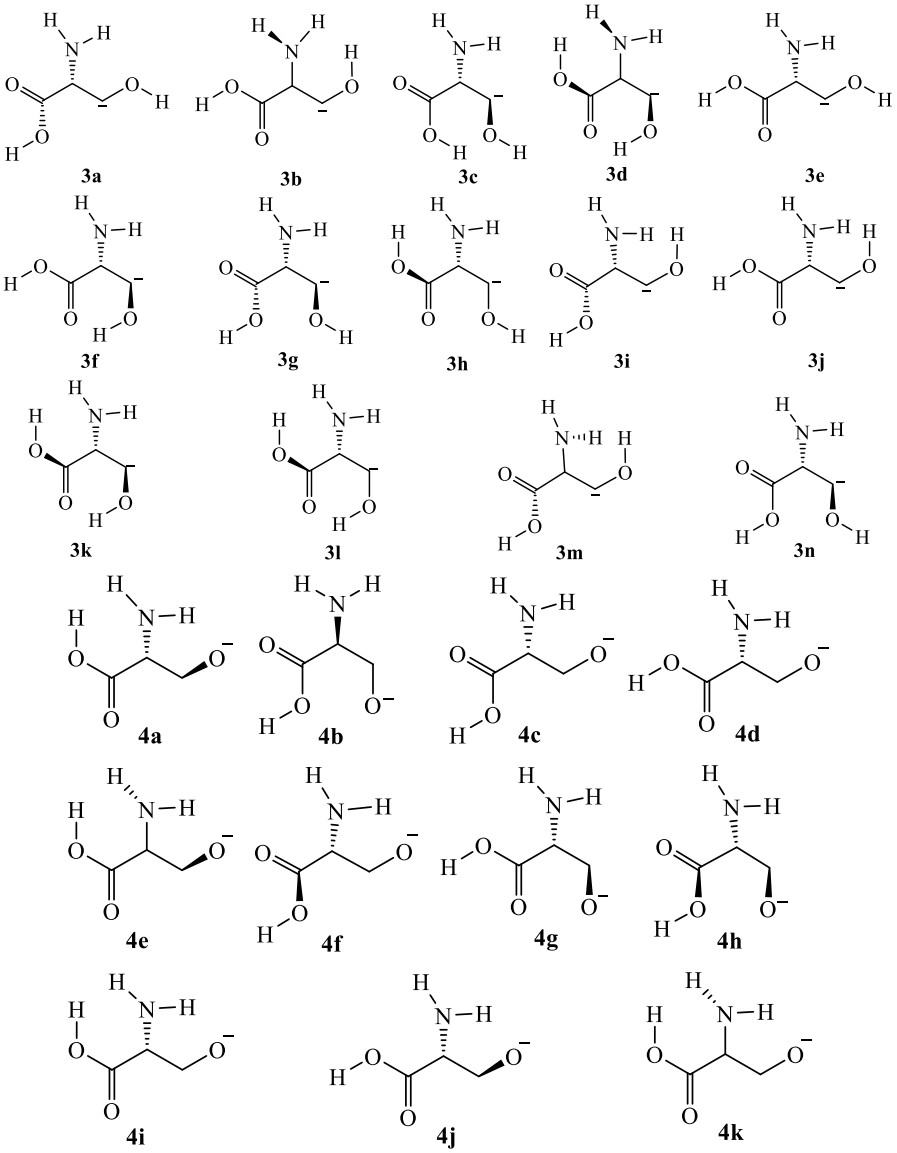

Figure 1: Schematic diagram of the four isomers of [Ser−H]$^-$

The structures of four species (46 species in total) of [Ser−H]$^-$ isomers are listed in Figure 1, and the associated energies are listed in Table 1. The enthalpy and Gibbs free energy of **1d** are both the lowest, so this structure is the most stable structure. The relative Gibbs free energies (ΔG) of other structures is calculated by taking **1d** as the zero point.

The ΔG of species **1** (**1a** ~ **1i**) ions are all lower than 11 kcal·mol^{-1}. This is because the negative charges are all on $-CO_2$, forming a relatively stable $-CO_2^-$ anionic group. In the $-CO_2^-$ group, there is a negative charge between the two oxygen atoms and the carbon atoms, and the conjugate system formed with the lone pair of oxygen atoms is relatively stable, so the energy of the first isomer is relatively low.

It can be seen from Figure 1 that the negative charges in all isomers of species **2** (**2a** ~ **2l**) are all located on α-C. For the negative charges on α-C cannot form an effective conjugate region like the negative charges on the terminal group, the energy of species **2** (31 ~ 42 kcal·mol^{-1}) is higher than that of species **1**. The negative charge of species **3** (**3a** ~ **3n**) is located on the β-C atom. From the results of energy range of isomers, it can be seen that the Gibbs free energy of species **3** (65.61 ~ 82.12 kcal·mol^{-1}) is higher than that of species **2**. The negative charge on β-C does not form an efficient conjugate region as the negative charge on the terminal group does, making species **3** higher in energy than species **2** and much higher than species **1**. The position of negative charge in species **4** (**4a**~**4k**) of ionic structure is on the hydroxyl group attached to β-C. From the energy range of isomers, it is found that the reaction of the fourth isomer has little difference with Gibbs free energy (33.86 ~ 46.22 kcal·mol^{-1}) and the reaction of the second isomer has little difference with Gibbs free energy (34.98 ~ 41.62 kcal·mol^{-1}).

3.2 NH_3-loss reaction of [Ser−H]$^-$

In this section, 6 kinds of [Ser−H]$^-$ isomers that can directly drop NH_3 molecules were obtained through optimization. The corresponding NH_3-loss reaction pathways (**Paths 1 ~ 6**) with dynamic barrier activation Gibbs free energies ($\Delta G^{\neq}$, kcal·mol^{-1}) and thermodynamic reaction Gibbs free energies ($\Delta_r G$, kcal·mol^{-1}) are shown in Figure 2.

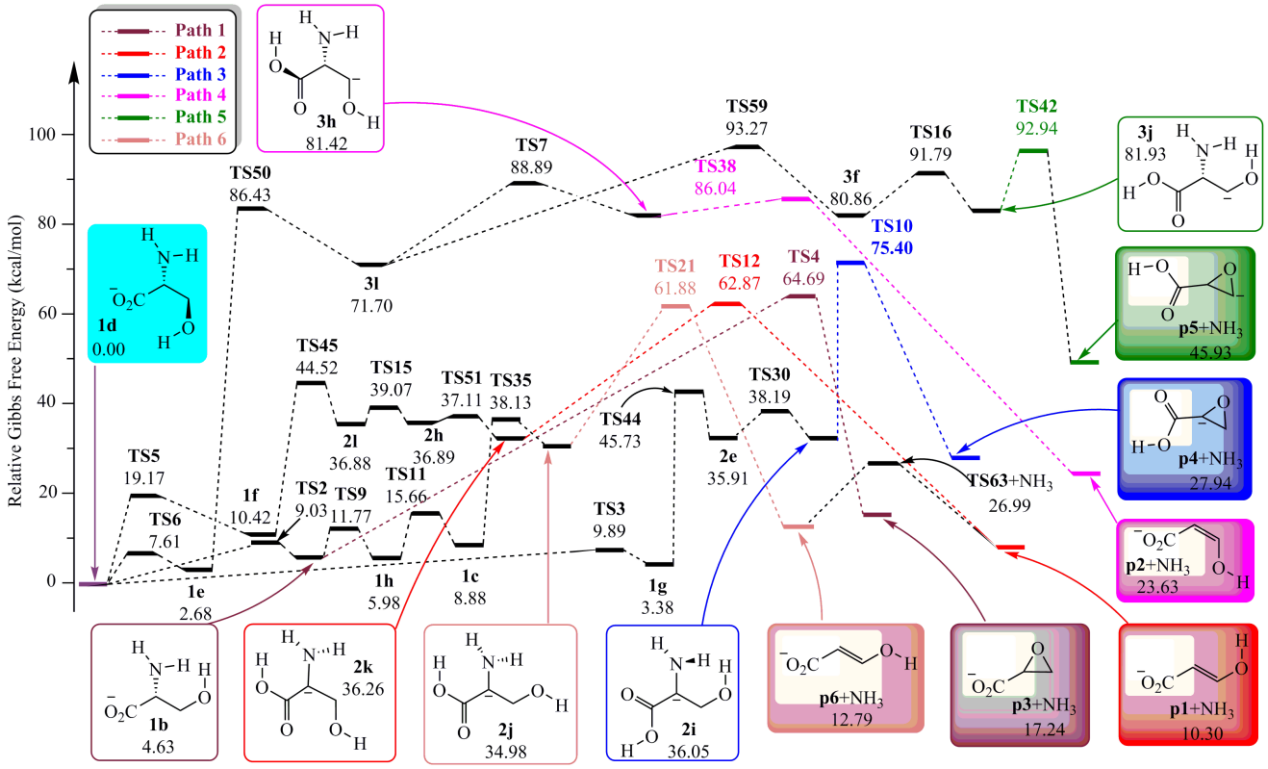

Figure 2: Potential energy profile of NH_3-loss reaction of [Ser−H]$^-$

In the potential energy profile of **Paths 1 ~ 6** of [Ser−H]$^-$ deamination reaction pathways given in Figure 2, there are five methods according to different deamination products. The first is the trans products **p1** and **p6** obtained by the cleavage of the [Ser−H]$^-$ ions **2j** and **2k**. The second is the *cis*- product **p2** obtained by the cleavage of the isomer **3h**. The third is the cleavage of the isomer **1b** under the experimental conditions, and the ternary ring **p3** ions including oxygen atoms are obtained. The fourth is the ternary ring **p4** ion containing oxygen atom obtained from the cleavage of isomer **2i**. And the fifth is the ternary ring **p5** ion containing oxygen atom obtained from the cleavage of isomer **3j**.

The $\Delta G^{\neq}$ of the transition states of the six [Ser−H]$^-$ deamination reaction pathways are **Path 1** (**TS4**, 64.69 kcal·mol^{-1}), **Path 2** (**TS12**, 62.87 kcal·mol^{-1}), **Path 3** (**TS10**, 75.40 kcal·mol^{-1}), **Path** 4 (**TS50**, 86.43 kcal·mol^{-1}), **Path 5** (**TS59**, 93.27 kcal·mol^{-1}), **Path 6** (**TS21**, 61.88 kcal·mol^{-1}). Among the six pathways, the $\Delta G^{\neq}$ of **Path 1**, **Path 2** and **Path 6** is lower than 65 kcal·mol^{-1}, while the $\Delta G^{\neq}$ of **Path 6** is the lowest, and the $\Delta G^{\neq}$ of the remaining three pathways is higher than 75 kcal·mol^{-1}. Among them, product fragment ions obtained after deamination of **Paths 3 ~ 5** are **p4** ($\Delta_r G$ = 27.94 kcal·mol^{-1}, $\Delta_r H$ = 42.36 kcal·mol^{-1}), **p2** ($\Delta_r G$ = 23.63 kcal·mol^{-1}, $\Delta_r H$ = 38.58 kcal·mol^{-1}) and **p5** ($\Delta_r G$ = 45.93 kcal·mol^{-1}, $\Delta_r H$ = 60.35 kcal·mol^{-1}), which energies is higher than the product ion **p3** ($\Delta_r G$ = 17.24 kcal·mol^{-1}, $\Delta_r H$ = 33.29 kcal·mol^{-1}) obtained by **Path 1**, and much higher than the products **p6** ($\Delta_r G$ = 12.79 kcal·mol^{-1}, $\Delta_r H$ = 27.80 kcal·mol^{-1}) and **p1** ($\Delta_r G$ = 10.30 kcal·mol^{-1}, $\Delta_r H$ = 25.02 kcal·mol^{-1}) of **Path 6** and **Path2**. Therefore, the reaction products **p1** and **p6** have high thermodynamic stability. Based on the lowest $\Delta G^{\neq}$ of **TS21**, the preferred NH_3-loss pathway given by theoretical study is **Path 6** (**1d→1b→1h→1c→2j→p6**+NH_3).

3.3 H_2O-loss reaction of [Ser−H]$^-$

In this section, 9 kinds of [Ser−H]$^-$ isomers that can directly drop H_2O molecules were obtained through optimization. The corresponding NH_3-loss reaction pathways (**Paths 7 ~ 15**) with dynamic barrier activation Gibbs free energies ($\Delta G^{\neq}$, kcal·mol^{-1}) and thermodynamic reaction Gibbs free energies ($\Delta_r G$, kcal·mol^{-1}) are shown in Figure 3 and Figure 4.

According to its isomerization process, H_2O-loss reaction pathways could be divided into 4 kinds, and the potential energy profiles are shown in Figure 3 and Figure 4 respectively. The first is a ternary ring **p7** ion containing an oxygen atom obtained by the cleavage of the isomer **1i**. The second is to obtain the ternary heterocyclic dehydrated ions **p8**, **p9** and **p15** containing

nitrogen atoms by cracking the isomers **2i**, **2h** and **2j**. The third is the cleavage of the isomers **3c**, **3m** and **3d** to obtain the four-membered ring **p12** ions containing oxygen atoms and the ternary ring **p10** and **p11** ions containing nitrogen atoms. The fourth is the ternary ring **p13** and **p14** ions containing nitrogen atoms obtained by the cleavage of isomers **4e** and **4k**.

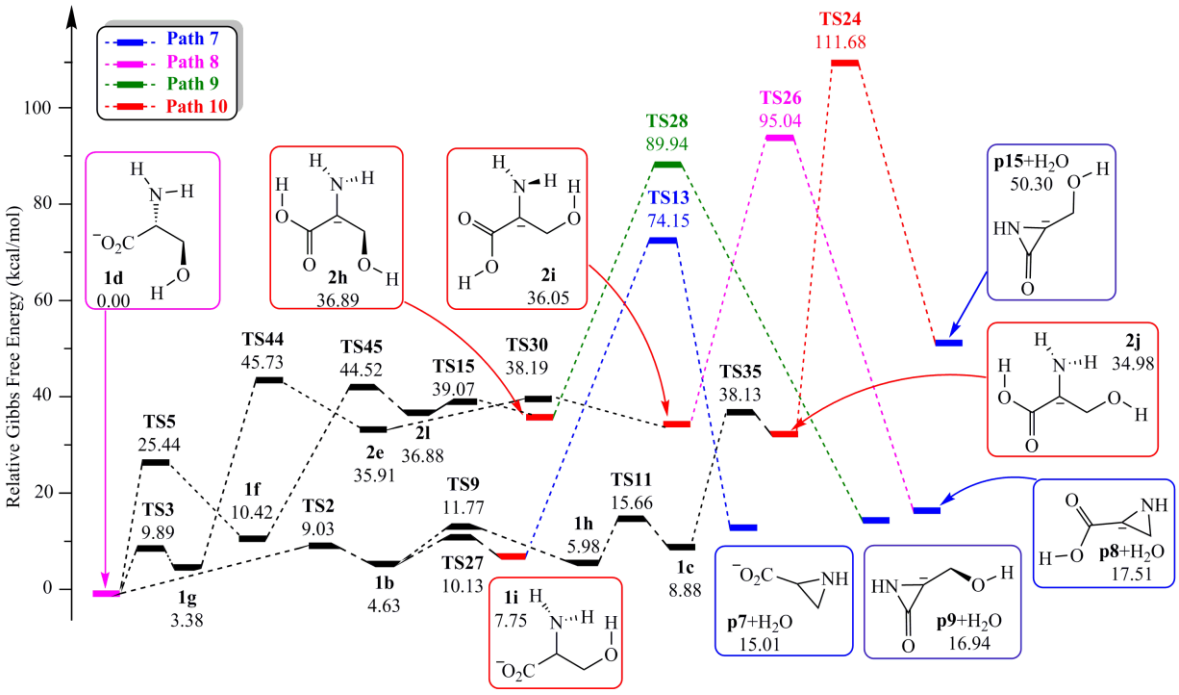

Figure 3: Potential energy profile (Paths 7 ~ 10) of H_2O-loss reaction of $[Ser-H]^-$

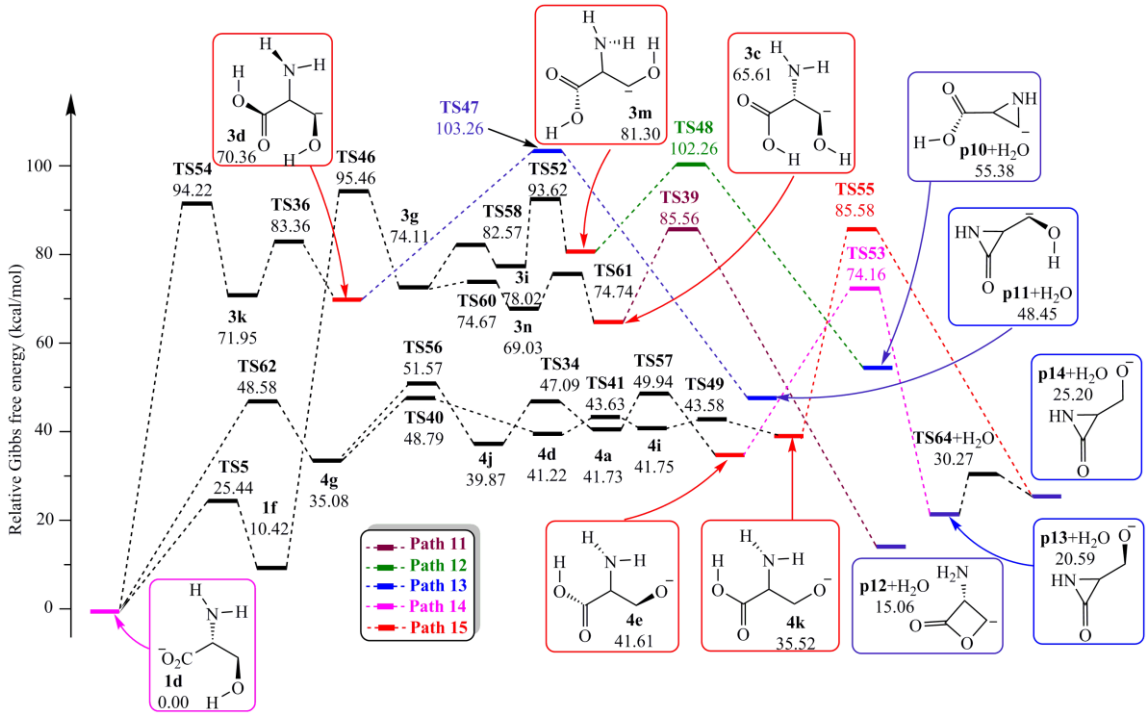

Figure 4: Potential energy profile (Paths 11 ~ 15) of H_2O-loss reaction of $[Ser-H]^-$

The $\Delta G^{\neq}$ of the rate-determine steps of transition states of 9 H_2O-loss pathways are **Path 7** (**TS13**, 74.15 kcal·mol^{-1}), **Path 8** (**TS26**, 95.04 kcal·mol^{-1}), **Path 9** (**TS28**, 89.94 kcal·mol^{-1}), **Path 10** (**TS24**, 111.68 kcal·mol^{-1}), **Path 11** (**TS46**, 95.46 kcal·mol^{-1}), **Path 12** (**TS48**, 102.26 kcal·mol^{-1}), **Path 13** (**TS47**, 103.26 kcal·mol^{-1}), **Path 14** (**TS53**, 74.16 kcal·mol^{-1}) and **Paths 15** (**TS55**, 85.58 kcal·mol^{-1}) respectively. Among the nine paths, only **Path 7**, **Path 14** and **Path 15** have activated Gibbs free energy lower

than 86 kcal·mol^{-1}, while the remaining six dehydration paths have activated Gibbs free energy higher than 89 kcal·mol^{-1}. Among them, **Path 7**, **Path 14** and **Path 15** were dehydrated to obtain product fragment ion **p7** (Δ_rG = 15.01 kcal·mol^{-1}, Δ_rH = 26.44 kcal·mol^{-1}), **p13** (Δ_rG = 20.59 kcal·mol^{-1}, Δ_rH = 34.01 kcal·mol^{-1}) and **p14**(Δ_rG = 25.20 kcal·mol^{-1}, Δ_rH = 37.78 kcal·mol^{-1}). According to the reaction kinetics, the $\Delta G^{\neq}$ values of **Path 7** and **Path 14** are similar to each other, and both can be carried out under the same conditions, which can become competitive paths. Therefore, in terms of thermodynamics, we can compare Δ_rG of products, because the product ion **p7** obtained by **Path 7** dehydration has the lowest energy and high thermodynamic stability. In the final theoretical study, the preferred H_2O-loss pathway is **Path 7** (**1d→1b→1i→p7**+H_2O).

4. CONCLUSION

In this paper, the mechanism of NH_3- and H_2O-loss of $[Ser{-}H]^-$ was studied at BH*and*HLYP/6-31G level. The details are listed below.

1. Through the analysis of the four kinds of $[Ser{-}H]^-$ isomers, it is found that the structure of the first kind of $[Ser{-}H]^-$ is the most stable, and its optimal structure is **1d**..
2. According to the calculation of NH_3-loss reaction of $[Ser{-}H]^-$, when the energy from the environment can provide over 62 kcal·mol^{-1}, NH_3-loss reaction will occur. The $\Delta G^{\neq}$ of **Path 6** is the lowest, and it is the most advantageous pathway.
3. According to the calculation of H_2O-loss reaction of $[Ser{-}H]^-$, when the energy from the environment can provide over 74 kcal·mol^{-1}, H_2O-loss reaction will happen. Among the products corresponding to the two paths in thermodynamics, the cyclic **p7** molecular ion has the lowest Δ_rG, which is the most dominant path among the H_2O-loss pathways.
4. In comparison, NH_3-loss is easier than H_2O-loss reaction in terms of kinetics and thermodynamics, and **Path 6** is the optimal reaction pathway for $[Ser{-}H]^-$ dissociation.

Fund project: "Three Longitudinal" Youth Innovative Talent Project of Heilongjiang Bayi Agricultural University (ZRCQC202010); Daqing City guiding science and technology project (zd-2021-88); Doctoral Research Foundation of Heilongjiang Bayi Agricultural University (XDB202112)

Author's brief introduction: Quan Sun (1990-), man, Master's Degree, Assistant laboratory Technician, Corresponding author, mainly engaged in theoretical study on the reaction mechanism of substances.

REFERENCE

1. National Health and Family Planning Commission of the P.R.C..WS/T 476—2015 Nutritional terms [Z]. 2015-12-29.
2. Zheng, G. (2016). Process optimization of efficient enzymatic conversion for L-serine and life cycleassessment [D]. *Huazhong University of Science and Technology*.
3. Tibbetts, A. S., & Appling, D. R. (2010). Compartmentalization of Mammalian folate-mediated one-carbon metabolism. *Annual review of nutrition*, *30*, 57-81.
4. Labuschagne, C. F., Van Den Broek, N. J., Mackay, G. M., Vousden, K. H., & Maddocks, O. D. (2014). Serine, but not glycine, supports one-carbon metabolism and proliferation of cancer cells. *Cell reports*, *7*(4), 1248-1258.
5. Bowie, J. H., Brinkworth, C. S., & Dua, S. (2002). Collision-induced fragmentations of the (M-H)− parent anions of underivatized peptides: An aid to structure determination and some unusual negative ion cleavages. *Mass Spectrometry Reviews*, *21*(2), 87-107.
6. Piraud, M., Vianey-Saban, C., Petritis, K., Elfakir, C., Steghens, J. P., Morla, A., & Bouchu, D. (2003). ESI-MS/MS analysis of underivatised amino acids: a new tool for the diagnosis of inherited disorders of amino acid metabolism. Fragmentation study of 79 molecules of biological interest in positive and negative ionisation mode. *Rapid Communications in Mass Spectrometry*, *17*(12), 1297-1311.
7. Eckersley, M., Bowie, J. H., & Hayes, R. N. (1989). Collision-induced dissociations of deprotonated peptides, dipeptides and tripeptides with hydrogen and alkyl α groups. An aid to structure determination. *Organic mass spectrometry*, *24*(8), 597-602.
8. Advances in Quantum Chemistry [J]. Advances in Quantum Chemistry, 2013, 65(4), 21-26.
9. Jia, B. (2013). Advances in quantum chemical computation [J]. *Science and Technology Innovation Herald*, (36), 14.
10. Su, Y., Li, W., Li, G., Ao, Z., & An, T. (2019). Density functional theory investigation of the enhanced adsorption mechanism and potential catalytic activity for formaldehyde degradation on Al-decorated C2N monolayer. *Chinese Journal of Catalysis*, *40*(5), 664-672.
11. Roothaan, C. C. J. (1951). New developments in molecular orbital theory. *Reviews of modern physics*, *23*(2), 69.
12. Pople, J. A., & Nesbet, R. K. (1954). Self-consistent orbitals for radicals. *The Journal of Chemical Physics*, *22*(3), 571-572.
13. McWeeny, R., & Diercksen, G. H. F. J. (1968). Self-consistent perturbation theory. II. Extension to open shells. *The Journal of Chemical Physics*, *49*(11), 4852-4856.
14. Hohenberg, P., & Kohn, W. (1964). Inhomogeneous electron gas. *Physical review*, *136*(3B), B864.-B871.
15. Kohn, W., & Sham, L. J. (1965). Self-consistent equations including exchange and correlation

effects. *Physical review*, *140*(4A), A1133-A1138.
16. Slater, J. C. (1974). The Self-Consistent Field for Molecular and Solids, Quantum Theory of Molecular and Solids, Vol. 4, McGraw-Hill, New York.
17. Vosko, S. H., Wilk, L., & Nusair, M. (1980). Accurate spin-dependent electron liquid correlation energies for local spin density calculations: a critical analysis. *Canadian Journal of physics*, *58*(8), 1200-1211.
18. Becke, A. D. (1988). Density-functional exchange-energy approximation with correct asymptotic behavior. *Physical review A*, *38*(6), 3098-3100.
19. Lee, C., Yang, W., & Parr, R. G. (1988). Development of the Colle-Salvetti correlation-energy formula into a functional of the electron density. *Physical review B*, *37*(2), 785-789.
20. Miehlich, B., Savin, A., Stoll, H., & Preuss, H. (1989). Results obtained with the correlation energy density functionals of Becke and Lee, Yang and Parr. *Chemical Physics Letters*, *157*(3), 200-206.
21. McLean, A. D., & Chandler, G. S. (1980). Contracted Gaussian basis sets for molecular calculations. I. Second row atoms, Z= 11–18. *The Journal of chemical physics*, *72*(10), 5639-5648.
22. Krishnan, R. B. J. S., Binkley, J. S., Seeger, R., & Pople, J. A. (1980). Self-consistent molecular orbital methods. XX. A basis set for correlated wave functions. *The Journal of chemical physics*, *72*(1), 650-654.
23. Frisch, M. J., Trucks, G. W., Schlegel, H. B., Scuseria, G. E., Robb, M. A., Cheeseman, J. R., ... & Fox, D. J. (2009). Gaussian 09, Revision D. 01, Gaussian, Inc., Wallingford CT. *See also: URL: http://www. gaussian. com*.